⑫

Amplitude Distribution of Cosmic Ray Events in Extrinsic IR Detectors

Prepared by

L. AUKERMAN
Electronics Research Laboratory
Laboratory Operations
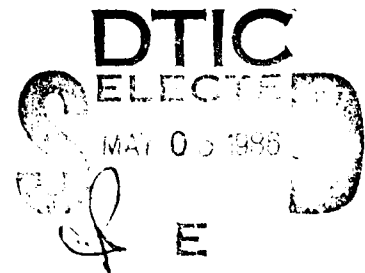The Aerospace Corporation
El Segundo, Calif. 90245

15 March 1986

DTIC
ELECTE
MAY 0 5 1986
E

AD-A167 692

Prepared for

SPACE DIVISION
AIR FORCE SYSTEMS COMMAND
Los Angeles Air Force Station
P.O. Box 92960, Worldway Postal Center
Los Angeles, CA 90009-2960

This report was submitted by The Aerospace Corporation, El Segundo, CA 90245, under Contract No. F04701-85-C-0086 with the Space Division, P.O. Box 92960, Worldway Postal Center, Los Angeles, CA 90009-2960. It was reviewed and approved for The Aerospace Corporation by M. J. Daugherty, Director, Electronics Research Laboratory.
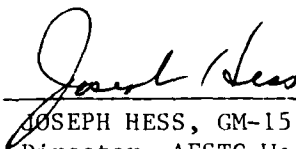
Lt Walter E. Leyland/YGJA was the Air Force project officer.

This report has been reviewed by the Public Affairs Office (PAS) and is releasable to the National Technical Information Service (NTIS). At NTIS, it will be available to the general public, including foreign nationals.

This technical report has been reviewed and is approved for publication. Publication of this report does not constitute Air Force approval of the report's findings or conclusions. It is published only for the exchange and stimulation of ideas.

WALTER E. LEYLAND, Lt, USAF
Project Officer
SD/YGJA

JOSEPH HESS, GM-15
Director, AFSTC West Coast Office
AFSTC/WCO OL-AB

REPORT DOCUMENTATION PAGE		READ INSTRUCTIONS BEFORE COMPLETING FORM
1. REPORT NUMBER SD-TR-86-17	2. GOVT ACCESSION NO. *AD-A167692*	3. RECIPIENT'S CATALOG NUMBER
4. TITLE *(and Subtitle)* AMPLITUDE DISTRIBUTION OF COSMIC RAY EVENTS IN EXTRINSIC IR DETECTORS		5. TYPE OF REPORT & PERIOD COVERED
		6. PERFORMING ORG. REPORT NUMBER TR-0086(6427-01)-1
7. AUTHOR(s) Lee Aukerman		8. CONTRACT OR GRANT NUMBER(s) F04701-85-C-0086
9. PERFORMING ORGANIZATION NAME AND ADDRESS The Aerospace Corporation El Segundo, Calif. 90245		10. PROGRAM ELEMENT, PROJECT, TASK AREA & WORK UNIT NUMBERS
11. CONTROLLING OFFICE NAME AND ADDRESS Space Division Los Angeles Air Force Station Los Angeles, Calif. 90009-2960		12. REPORT DATE 15 March 1986
		13. NUMBER OF PAGES 21
14. MONITORING AGENCY NAME & ADDRESS*(If different from Controlling Office)*		15. SECURITY CLASS. *(of this report)* Unclassified
		15a. DECLASSIFICATION/DOWNGRADING SCHEDULE

16. DISTRIBUTION STATEMENT *(of this Report)*

Approved for public release; distribution unlimited.

17. DISTRIBUTION STATEMENT *(of the abstract entered in Block 20, if different from Report)*

18. SUPPLEMENTARY NOTES

19. KEY WORDS *(Continue on reverse side if necessary and identify by block number)*

Cosmic Rays
IR Detectors
Single Events

20. ABSTRACT *(Continue on reverse side if necessary and identify by block number)*

A method of calculating the amplitude distribution of cosmic ray events in
IR detectors utilizing known range-energy relationships for the various
cosmic particles (mostly protons and helium nuclei) and published cosmic ray
energy spectra is described. Good agreement is obtained between the calcu-
lated amplitude distribution and the spurious events observed in an
extrinsic detector during a flight test.

DD FORM 1473
(FACSIMILE)

CONTENTS

1

FIGURES

I. INTRODUCTION

Because of their very large volume and extreme sensitivity, extrinsic infrared detectors[1] operating above the atmosphere may be quite vulnerable to single ionization events resulting from energetic ionized particles in space. This paper describes a method of applying existing techniques for calculating the intensity distribution of false signals resulting from cosmic rays as they impinge upon a silicon detector of given dimensions. The result is a plot of the amplitude distribution expected from near earth cosmic ray events. The program can also make comparisons of various shielding models and the effects of different particles and particle spectra.

II. SPHERICALLY SYMMETRIC SHIELDING MODEL

Figure 1 illustrates how the "straight ahead" approximation is used to determine the particle flux inside a spherical cavity. Data from range-energy tables are functionalized by means of an interpolation program yielding R(E), range as a function of energy, and its inverse, E(R). Then

$$E_1 = E(R(E_2) + T_s) \qquad (1)$$

where E_1 is the energy of the particle incident on the shield and E_2 is the energy of this particle after it is degraded by the shield thickness T_s. Equation (1) is also the basis for determining deposited energy in the sensitive region of the detector. The degraded flux spectrum, which for spherical geometry is assumed to be the flux incident on the detector, becomes

$$\Phi_2(E_2) = \Phi_1(E_1) \times (dE_1/dE_2) \qquad (2)$$

where $\Phi_1(E_1)$ is the flux spectrum incident on the shield as obtained in this case from the work of Adams et. al.[2], and the derivative (dE_1/dE_2) is obtained from Eq. (1).

The effects of shielding on the proton and helium spectra are illustrated in Figures 2 and 3, respectively, for two widely different shielding thicknesses. Note that once the very low energy component is removed, the shield thickness has little effect on the spectrum.

Secondaries coming from the shield were neglected in this calculation. There are two sources of secondaries to be considered: (1) those resulting from nuclear reactions between the incident energetic nuclei and the nuclei of the shield material, and (2) those resulting from hot electrons produced by the highly ionized tracks of the incident nuclei. The cross sections for nuclear reactions are known and indicate this source of secondary generation to be negligible compared to the primary particle event rate. No attempt was made to estimate the secondaries resulting from hot electrons but it seems reasonable that such events if present would produce only low energy or low magnitude pulses.

7

T$_s$ SHIELD THICKNESS

Φ_1 = OMNI DIRECTIONAL FLUX OUTSIDE SHIELD (No. /(cm^2-ster-MeV-sec))

DETECTOR

Φ_2

R(E) = RANGE vs ENERGY

E(R) = ENERGY vs RANGE

Φ_2 = OMNI DIRECTIONAL FLUX INSIDE SHIELD (No. /(cm^2-ster-MeV-sec))

$$\Phi_2(E_2) = \Phi_1(E_1) \times (dE_1 / dE_2)$$
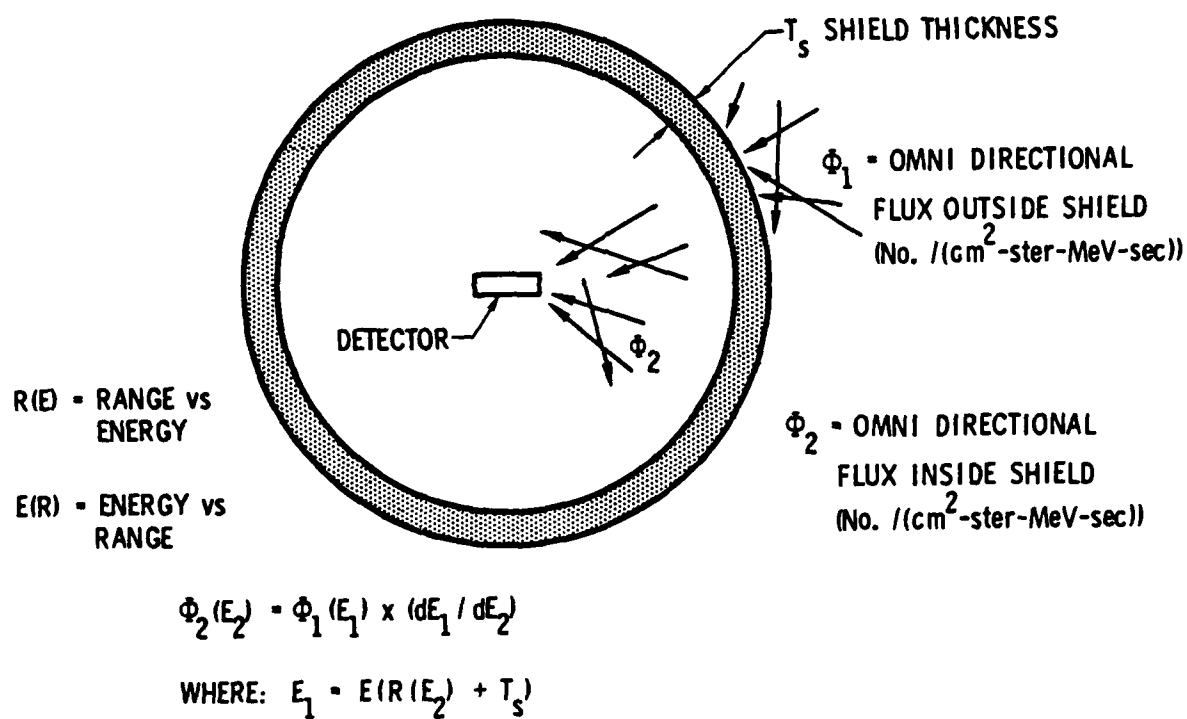
$$\text{WHERE: } E_1 = E(R(E_2) + T_s)$$
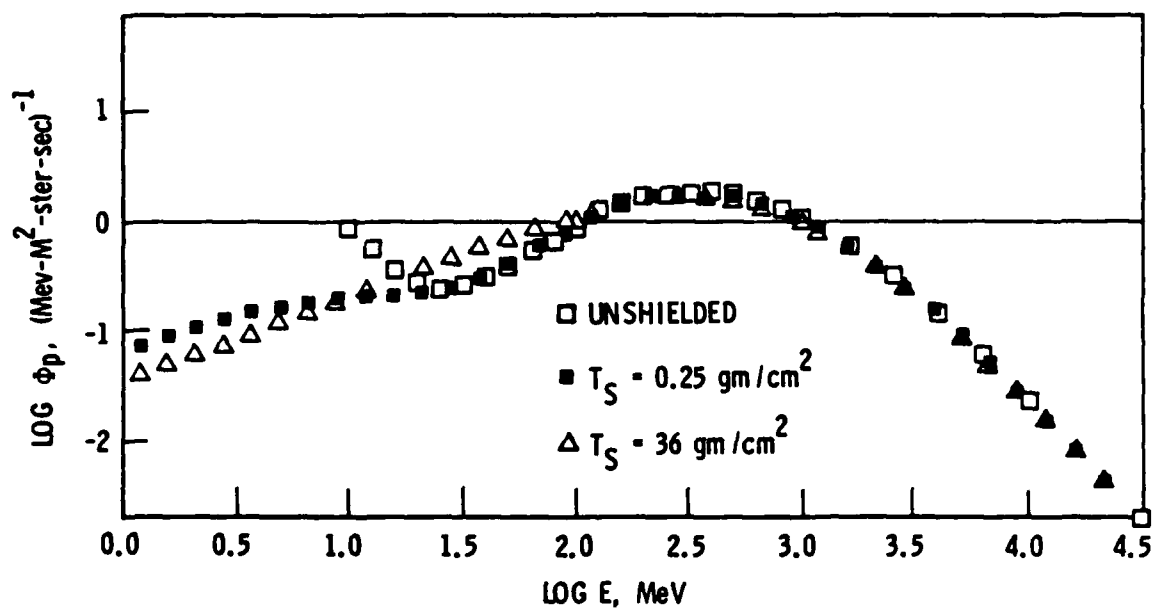
Figure 1. Spherically Symmetric Shielding Model

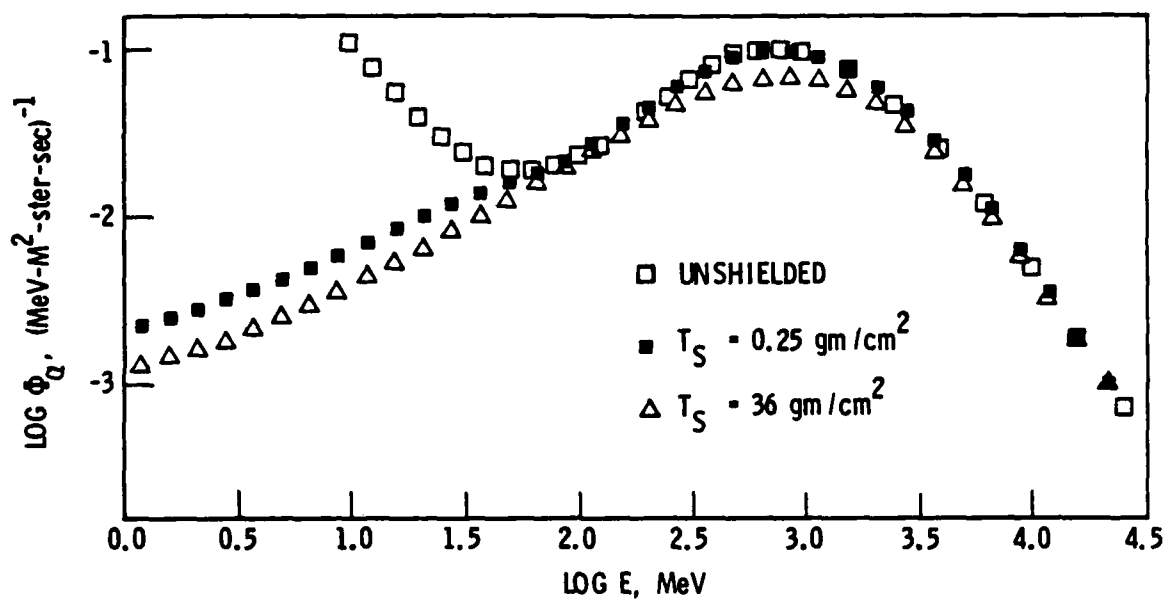Figure 2.   Proton Spectrum—Solar Min: the Effect of Shielding

Figure 3. Helium Spectrum-Solar Min: the Effect of Shielding

III. DEPOSITED ENERGY

The omnidirectional particle flux inside the shield creates tracks of highly ionized regions (hole-electron pairs) in the detector. Essentially all of the energy deposited within the sensitive volume of the detector creates hole-electron pairs (one pair per 3.6 eV) which are collected and amplified by the electronics to produce an output pulse. To get a pulse height distribution we first determine the deposited energy distribution.

Consider the minimal event which we define as the passage of a proton of energy E_{min}, corresponding to the minimum in (dE/dx), perpendicularly through the smallest dimension of the parallelepiped shaped sensitive volume. Then the resulting deposited energy corresponds to the energy of the maximum of the deposited energy histogram. For protons dE/dx at E_{min} is 1.7 MeV-cm^2/gm. The deposited charge in Coulombs is (dE/dx $\times$ 10^6 $\times$ s $\times$ 1.6 $\times$ 10^{-19}/3.6) = (7.56 $\times$ 10^{-14} $\times$ s) where, in this case, s, the chord length in gm/cm^2, is the thickness of the detector. For a 100 μm thick (0.0233 gm/cm^2) extrinsic detector, the minimal event deposits a charge of 1.76 $\times$ 10^{-3} pC, or about 10^4 e.h. pairs. This is quite large compared to many infrared signals likely to be encountered. Assume the pulse is amplified by a conventional trans-impedance amplifier (TIA) as in Figure 4. Since the pulse is very fast, it can be shown that the output of the TIA is $V_o \cong Q/C_{FB}$, i.e., the deposited charge divided by the feedback capacitance. For C_{FB} = .01 pf V_o is about 0.2 volt, much larger than the usual sources of noise.

Calculations of single event rates for microelectronics invariably assume that the deposited energy is (LET) $\times$ (chord length, s, of the track through the sensitive volume). LET, the linear energy transfer, is dE/dX. This "LET approximation" is quite safe for microelectronics because of the very small dimensions involved. For IR detectors, in some cases hundreds of microns thick, the LET approximation may well be inadequate. Thus, for the present calculations, the average deposited energy $\overline{DE}$ is computed from the range-energy relation for each component of the cosmic background:

11
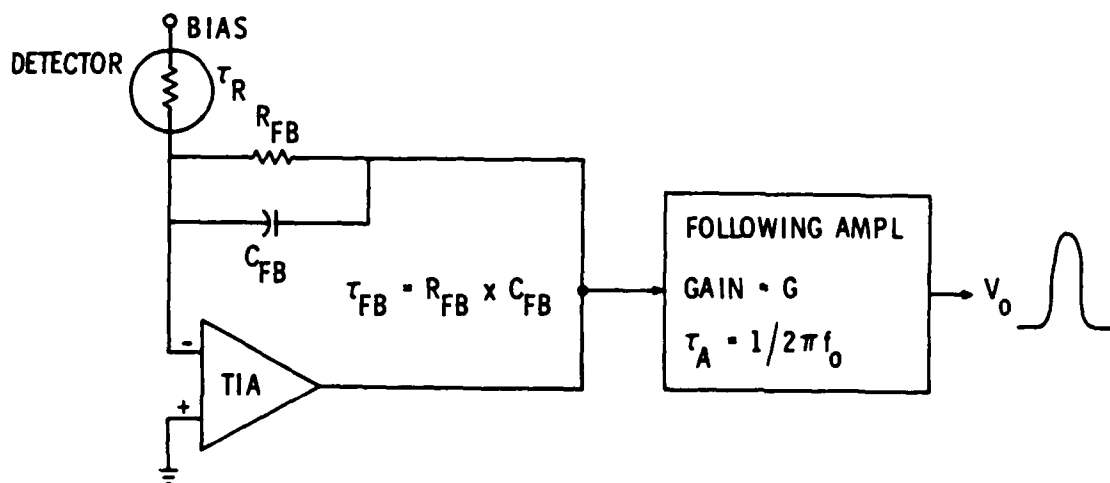
$$V_o = \frac{GQ}{C_{FB}} V_{norm} , \quad Q = 4.44 \times 10^{-20} \times DE$$

$$V_{norm} = Z^{-\left[Z/(Z-1)\right]} , \quad Z = \tau_A / \tau_{FB} , \text{ FOR } \tau_R \ll \tau_{FB} \text{ OR } \tau_A$$

Figure 4. Typical Detector with Trans-Impedance Amplifier

12

$$\overline{DE} = \begin{cases} E_2, & \text{for } E_2 < E(s) \\ E_2 - E(R(E_2)-s), & \text{for } E_2 > E(s) \end{cases} \qquad (3)$$

where E_2 is the energy of the particle after it has been degraded by the shield, but before it has entered the detector. Note that the total incident energy, E_2, is deposited in the detector if it is less than the energy required for a range of s. If E_2 is greater than this the particle will escape the sensitive region and $\overline{DE}$ is E_2 minus the energy of the particle as it escapes from the sensitive region. To account for collection of charge by diffusion one may add a small amount to the dimensions of the detector to estimate its effective dimensions. This has not been done in the present calculations.

Figures 5 and 6 plot $\overline{DE}$ (E_2) for two widely differing values of s: 0.1 and 1.75 gm/cm^2, respectively. Also plotted with the dashed line is the LET approximation (s × dE/dx). It is seen that the LET approximation is very good for those protons that are not stopped within the sensitive volume. But for those stopped ($E_2 < E(s)$) the LET approximation greatly overestimates the deposited energy. For s = 0.1 gm/cm^2, there are very few protons of energy $E_2 < E(s)$ = 6.6 Mev (.02%). For s = 1.75 gm/cm^2 about 0.2% of the incident protons are less energetic than E(s) = 4.0 MeV (see Figure 6). Thus, using the LET approximation could affect the shape of the pulse height histogram in the very large pulse height region if the dimensions of the sensitive volume are large enough. If the maximum chord length is less than about 0.75 cm (1.75 gm/cm^2) the LET approximation should be reasonably accurate. In the present calculations, however, the more accurate method (Eq. (3)) is retained for purposes of generality.
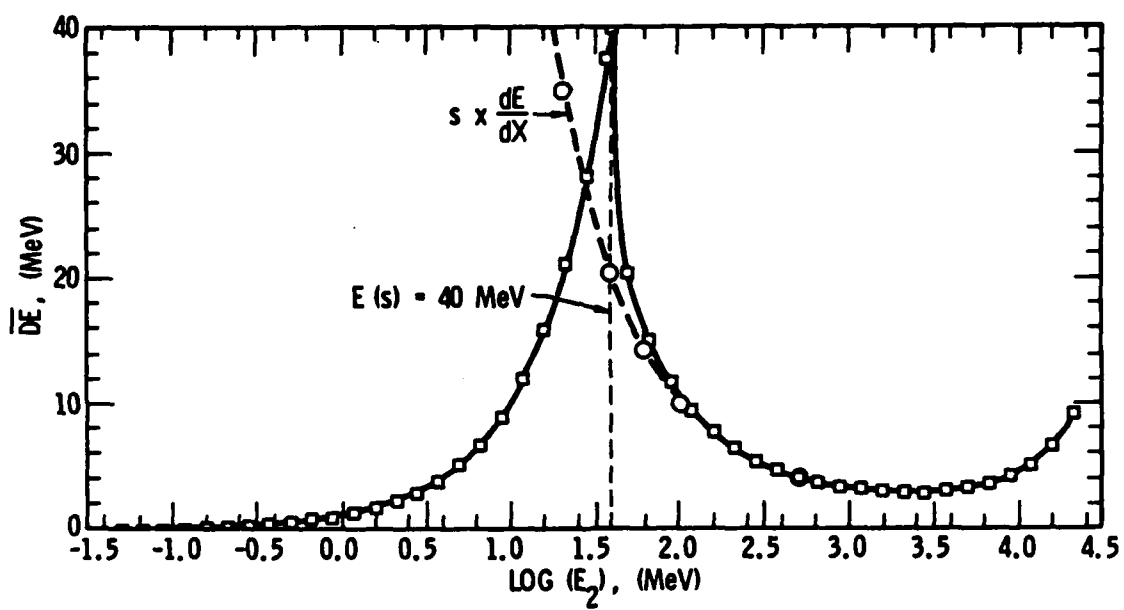
Figure 5. $\overline{DE}$ vs log (E_2): $s = 0.1$ gm/cm^2 (0.043 cm)

14

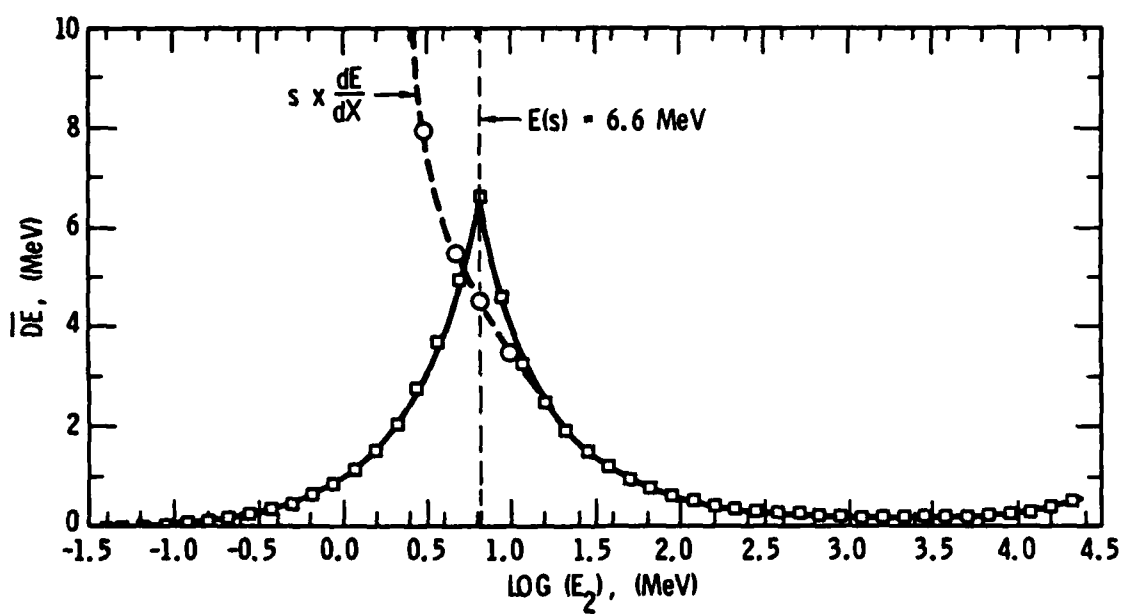Figure 6. $\overline{DE}$ vs log (E_2): s = 1.75 gm/cm^2 (0.75 cm)

15

IV. AMPLITUDE DISTRIBUTION FUNCTIONS

The function $\overline{DE}$ (E_2) for a given chord length s through the sensitive volume can always be divided into three monotonic intervals: $\left(0 < E_2 < E(s)\right)$, $(E(s) < E_2 < E_{min})$, and $(E_2 > E_{min})$. (In Figures 5 and 6 the minimum in $\overline{DE}$ corresponds to E_{min}.) Let N_s (DE) be the deposited energy distribution for a given s; i.e., N_s (DE) × ΔDE is the number of events/cm^2-ster that deposit energy in the range DE to (DE + ΔDE). Thus, the contribution to N_s(DE) by the ith interval is:

$$N_{si}(DE) \times |\Delta DE| = \int_{E_{2L}}^{E_{2U}} \Phi_2(E_2) \, dE_2 \tag{4}$$

where E_{2L} and E_{2U} are, respectively, solutions of Eq. (3), as follows:

$$DE = \overline{DE} \ (E_{2L}, s)$$

$$DE + \Delta DE = \overline{DE} \ (E_{2U}, \ s) \tag{5}$$

Equation (4) assumes that the probability, P(DE), of depositing energy DE is a delta function: $P(DE) = \delta \ (DE - \overline{DE})$. This is a very safe assumption for protons and heavier particles. The total contribution is the sum of the three; $N_s(DE) = \Sigma N_{si}(DE)$ provided the ΔDE intervals are the same. For the total distribution N_j(DE) of deposited energy produced by the jth component we utilize the exact chord length distribution of Petroff[3], F_s, as follows:

$$N_j(DE) = 4\pi \times \overline{A}_p \times \int_0^{S_{max}} N_s(DE) \times F_s \, ds \tag{6}$$

where $\overline{A}_p$ is the average projected area of the sensitive volume and S_{max} is its largest chord length:

$$S_{max} = (L^2 + W^2 + H^2)^{0.5} \tag{7}$$

17

where L, W, H are, respectively the length, width and height of the parallele-piped shaped sensitive volume. The total distribution is the sum of those produced by individual components: $N(DE) = \sum_j N_i(DE)$. In the present calcula-tion we considered protons and helium only. In other calculations we found that the inclusion of heavier elements make no noticeable difference. The cumulative distribution is

$$CN(DE) = \int_{DE}^{DE(S_{max})} N(DE) \times dDE \qquad (8)$$

One can calculate the total number of cosmic ray particles per cm^2 of average projected area that penetrate the sensitive region by integrating Adam's spectra (after a moderate amount of shielding). This gives 1.64 events/cm^2sec and agrees quite well with CN(0) obtained from Equation (8), confirming the internal consistency of the calculation.

To convert Eq. (8) to output voltage distribution, $N(V) = N(DE) \times \left(\frac{dV}{d(DE)}\right)^{-1}$ where the peak output voltage, V, is obtained from linear circuit theory for the circuit of Figure 4:

$$V = \frac{GQ}{C_{FB}} V_{norm} \qquad (9)$$

where C_{FB} is the capacitance across the feedback resistor, R_{FB}, of the TIA, G is the D.C. gain of the following amplifiers, and Q is the collected charge: $Q = 4.44 \times 10^{-20} \times (DE)$. From linear circuit theory, V_{norm} can be determined as a function of τ_R, τ_{FB}, and τ_A, which are respectively the response time of the detector (carrier lifetime), $R_{FB} C_{FB}$, and $1/2\pi f_o$, where f_o is the roll off frequency of the following amplifiers. If τ_R is very small compared to the smaller of τ_{FB} and τ_A (which is usually the case) then

$$V_{norm} = Z^{-[Z/(Z-1)]} \qquad (10)$$

where, $Z = \tau_A/\tau_{FB}$. The derivative $\frac{dV}{d(DE)}$ is obtained from Eq. (9).

Equation (10) is plotted in Figure 7 to show its monotonic behavior. Thus to decrease the effect of the spurious cosmic ray pulses one should increase the amplifier's response time and decrease the parasitic capacitance across the feedback resistor of the TIA as much as possible without loss of signal amplitude. This requires keeping τ_A less than the dwell time or the pulse width of the optical signal.

In Figure 8 the cumulative amplitude distribution calculated for an array of extrinsic detectors shielded with 62 gm/cm^2 of high Z material is plotted as a function of amplitude in arbitrary units. (An array of N identical detectors would have an event rate of N times that of a single detector.) This array has also been flight tested at low orbit where Van Allen radiation can be neglected, but above the earth's atmosphere. Thus, a likely candidate for the cause of fast, spurious output pulses would be near earth cosmic rays. The effect of earth shielding was taken into consideration by assuming exposure to only 2π steradians of omnidirectional cosmic rays. The cumulative amplitude distribution of "fast, spurious" output pulses obtained during the flight test is also plotted in Figure 8 against the same scale. Considering the uncertainty in particle fluxes, the agreement is very good, except at low pulse heights where the calculated values are too low. This might be the result of secondaries produced in the thick shield since these secondaries were not included in the calculation and are expected to lie in the low amplitude region.
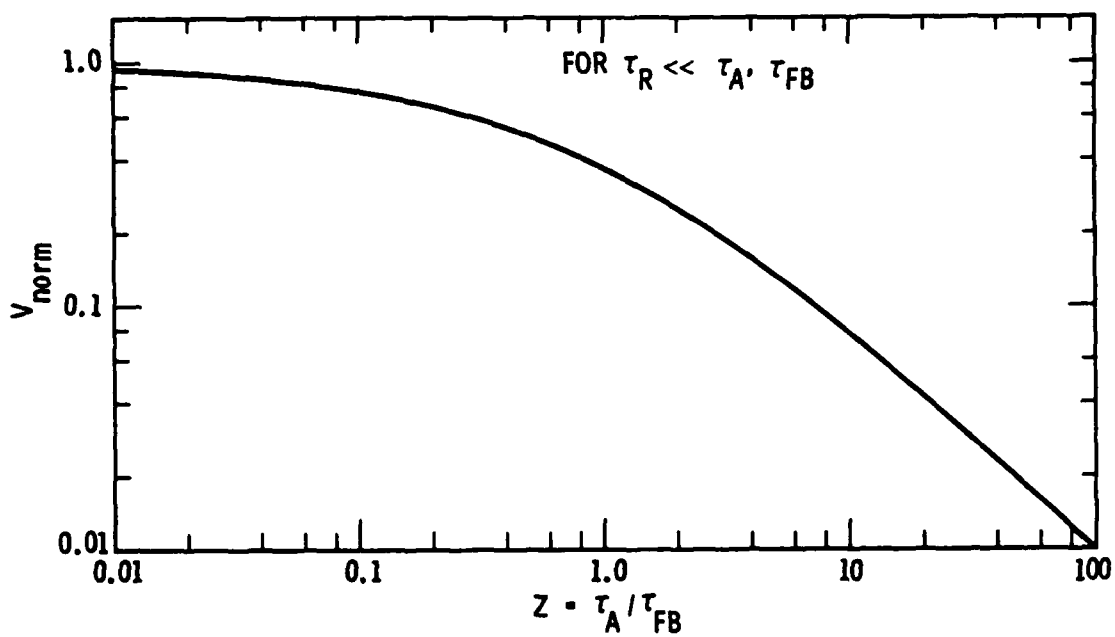
Figure 7. V_{norm} vs $Z(= \tau_A/\tau_R)$. τ_A = Amplifier Response Time, τ_{FB} = Feedback Time Constant, and τ_R = Response Time for the Detector
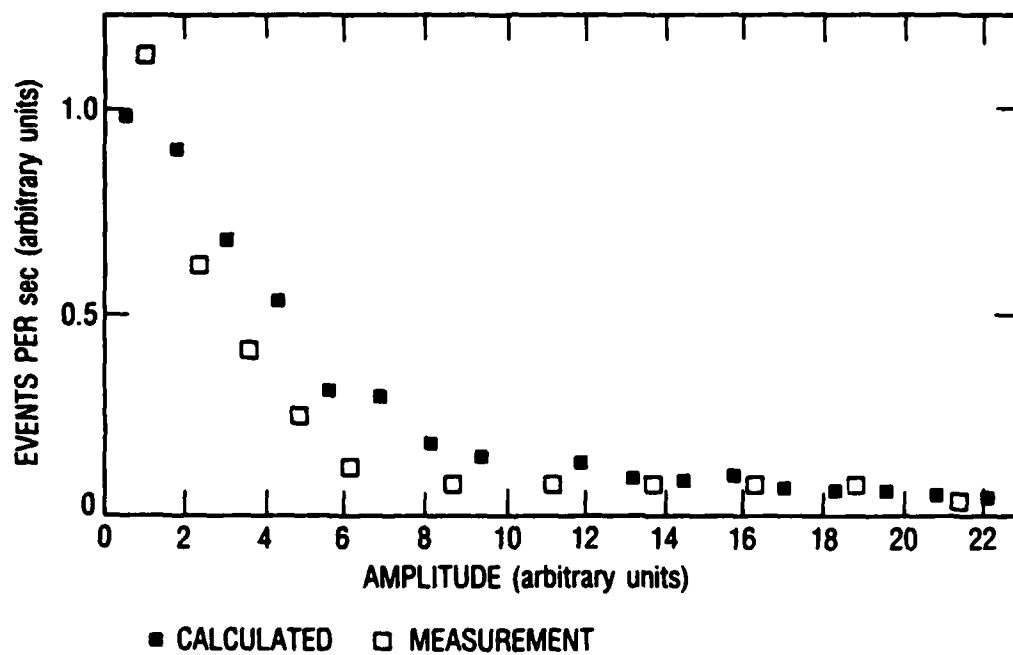
Figure 8. Cumulative Amplitude Distribution of Cosmic Ray Events

V. CONCLUSIONS

Good agreement was obtained between the calculated amplitude distribution of cosmic ray events and the spurious events observed in an extrinsic detector during a flight test below the Van Allen radiation belts. The date of the flight was taken into consideration according to the recipe described by Adams[2]. Although the deposited energy was determined from the range-energy relation it appears that the LET approximation would be adequate for detectors whose maximum dimension is less than 0.75 cm. A method of decreasing the amplitude of these pulses by taking advantage of their fast risetime was described.

REFERENCES

[1] Peter R. Bratt, "Impurity Germanium and Silicon Infrared Detectors," Semiconductors and Semimetals, R. K. Willardson and A. C. Beer, eds., Academic Press, New York (1977) Vol. 12, pp. 39-142.

[2] J. H. Adams, Jr., R. Silberberg, and C. H. Tsao, "Cosmic Ray Effects on Microelectronics, Part I: The Near-Earth Particle Environment," NRL Memorandum Report 4506, Naval Research Laboratory, Washington, DC (August 25, 1981).

[3] James C. Pickel and James T. Blandford, Jr., IEEE Trans. Nucl. Sci., NS-27 (No. 2), 1006 (1980).

The Aerospace Corporation functions as an "architect-engineer" for national security projects, specializing in advanced military space systems. Providing research support, the corporation's Laboratory Operations conducts experimental and theoretical investigations that focus on the application of scientific and technical advances to such systems. Vital to the success of these investigations is the technical staff's wide-ranging expertise and its ability to stay current with new developments. This expertise is enhanced by a research program aimed at dealing with the many problems associated with rapidly evolving space systems. Contributing their capabilities to the research effort are these individual laboratories:

Aerophysics Laboratory: Launch vehicle and reentry fluid mechanics, heat transfer and flight dynamics; chemical and electric propulsion, propellant chemistry, chemical dynamics, environmental chemistry, trace detection; spacecraft structural mechanics, contamination, thermal and structural control; high temperature thermomechanics, gas kinetics and radiation; cw and pulsed chemical and excimer laser development including chemical kinetics, spectroscopy, optical resonators, beam control, atmospheric propagation, laser effects and countermeasures.

Chemistry and Physics Laboratory: Atmospheric chemical reactions, atmospheric optics, light scattering, state-specific chemical reactions and radiative signatures of missile plumes, sensor out-of-field-of-view rejection, applied laser spectroscopy, laser chemistry, laser optoelectronics, solar cell physics, battery electrochemistry, space vacuum and radiation effects on materials, lubrication and surface phenomena, thermionic emission, photo-sensitive materials and detectors, atomic frequency standards, and environmental chemistry.

Computer Science Laboratory: Program verification, program translation, performance-sensitive system design, distributed architectures for spaceborne computers, fault-tolerant computer systems, artificial intelligence, micro-electronics applications, communication protocols, and computer security.

Electronics Research Laboratory: Microelectronics, solid-state device physics, compound semiconductors, radiation hardening; electro-optics, quantum electronics, solid-state lasers, optical propagation and communications; microwave semiconductor devices, microwave/millimeter wave measurements, diagnostics and radiometry, microwave/millimeter wave thermionic devices; atomic time and frequency standards; antennas, rf systems, electromagnetic propagation phenomena, space communication systems.

Materials Sciences Laboratory: Development of new materials: metals, alloys, ceramics, polymers and their composites, and new forms of carbon; non-destructive evaluation, component failure analysis and reliability; fracture mechanics and stress corrosion; analysis and evaluation of materials at cryogenic and elevated temperatures as well as in space and enemy-induced environments.

Space Sciences Laboratory: Magnetospheric, auroral and cosmic ray physics, wave-particle interactions, magnetospheric plasma waves; atmospheric and ionospheric physics, density and composition of the upper atmosphere, remote sensing using atmospheric radiation; solar physics, infrared astronomy, infrared signature analysis; effects of solar activity, magnetic storms and nuclear explosions on the earth's atmosphere, ionosphere and magnetosphere; effects of electromagnetic and particulate radiations on space systems; space instrumentation.

END
FILMED

6-86

DTIC